01,07

Multifractal properties of the molybdenum ribbon surface at mechanical loading

© B.A. Obidov, V.E. Korsukov, V.L. Hilarov, A.V. Ankudinov, P.N. Butenko, S.A. Knyazev, M.M. Korsukova

Ioffe Institute,
St. Petersburg, Russia

E-mail: Barzu.Obidov@mail.ioffe.ru

Received April 26, 2022
Revised April 26, 2022
Accepted May 2, 2022

The effect of uniaxial tensile stress on the atomic structure and relief of the subsurface layer of molybdenum ribbons has been studied. The destruction of the Mo (100) face with the formation of crystallites was revealed near the crack tip. At the same time, the block structures are found to rotate both in the lateral plane and in its perpendicular plane. The surface layer structure in the lateral plane of the ribbon is fragmented into sections, which is associated with the surface relief at different scales. With a help of the concept of multifractal formalism, the spectra of singularities of the initial, loaded and ruptured surface are calculated. It is found that the width of the singularity spectrum, can serve as an indication of the forthcoming rupture..

Keywords: molybdenum ribbon, mechanical load, annealing, destruction of material, block structures, surface, multifractal formalism.

DOI: 10.21883/PSS.2022.08.54606.364

1. Introduction

At present, there is an intensive growth in research into the creation of nanomaterials and the development of nanotechnologies. This is because nanomaterials have qualitatively new properties, functional and performance characteristics that differ significantly from those of macroscopic objects [1–3]. The functional properties of such materials are of interest in terms of hetero-catalysis, sensorics, microelectronics and much more [4–7]. One of the methods of obtaining nanomaterials is the dispersion of macroscopic solids, in which their mechanical, thermal, chemical (or joint) destruction occurs. By disintegrating, the sample, in particular its surface, may contain nanoscale clusters, respectively, partially or completely, may be a nanomaterial whose properties will differ from the original macroscopic object. The dispersion process can be accompanied by a transformation of the atomic structure and surface topography of materials.

In refs [8,9], changes in the atomic structure and surface relief of thin platinum foil during recrystallization and uniaxial stretching under Ultra High Vacuum (UHV) conditions were studied. The results obtained have been used to detail the mechanisms of plastic deformation and nucleation of fracture in metals with FCC-lattice, as well as to purposefully modify the surface morphology to solve specific problems of nanoelectronics and optical spectroscopy.

Metals with a BCC-lattice, such as molybdenum, have a different type of dislocation structures, a different set of sliding planes, and, accordingly, different mechanisms of recrystallization, deformation, and fracture. Mo and its compounds in the form of thin film structures are widely used in nanoelectronics for creating heteroepitaxial planar structures, solar cells, etc. [10,11]. Therefore, it is of undoubted interest to study the structure of near-surface layers of metals with BCC-lattice — such as molybdenum under temperature and mechanical influences. Certain results of studies of the structure of molybdenum bands under external impact were presented in [12–14], however, the behavior of the near-surface layers under pre-breaking load has been poorly studied.

Statistical methods, using space self-similarity of the surface relief, considering collective behavior of inhomogenities of the surface relief, are widely used nowadays. One such method is the Multifractal Formalism Conception (MFFC) [15]. Having the geometric parameters of the surface topography obtained, for example, by Scanning Probe Microscopy (SPM) methods, applying this concept, it is possible to describe the current state of the material surface and its behavior trends under external impact [16,17]. In ref. [18], the nanostructures formed as multiscale Pt diffraction lattices by thermomechanical action were considered as a fractal object. The relief anisotropy and the ability of these objects to function at different scales was quantified by calculating the components of fractal dimensionality (D_f) relative to the position of the corrugations. By the value of D_f, we can judge a measure of the characteristics of the surface topography, including its smoothness, however, the surfaces of real materials are heterogeneous and anisotropic, hence, the details of local scaling must be taken into account. Singularity spectra, obtained via MFFC formalism is suitable in this case and was used in [19] while studying Pt foil. No such

consideration has yet been made with respect to Mo, as far as we know.

The purpose of this paper is to interpret, using the MFFC method, the effect of stretching on the atomic structure and surface topography of metal with BCC-lattice — molybdenum under uniaxial tension and to establish the signs of incoming rupture.

2. Materials and research techniques

A molybdenum band of $20\,\mu$m thickness was chosen as the test material, from which 30 mm long and 3 mm wide samples were cut. Radial stress concentrators (in the form of semicircular notches) with a radius of $r = 1$ mm were created on the large sides of the samples. Next the surface of the samples was cleaned by treatment in acetone and isopropyl alcohol followed by drying in dry nitrogen. After that, the samples were attached to an uniaxial stretching device, which was placed in a vacuum chamber of the Low Energy Electron Diffraction (LEED) diffractometer, where they were further processed and recrystallized by high-temperature heating in a vacuum and oxygen atmosphere. The UHV sample surface preparation procedure is described in [14].

The LEED method using the VARIAN facility was used to monitor *in situ* the transformation of the atomic surface structure of the samples, including integral patterns (Integral (Int-LEED)) [20], during recrystallization and uniaxial stretching (up to rupture) in UHV.

The surface topography of the Mo-bands was studied by Atomic-Force Microscopy (AFM) on the Integra Aura device in tapping mode before and after uniaxial tension (up to the moment of sample rupture). We studied samples that had already been recrystallized in the LEED diffractometer chamber but had not been stretched. In order to study *in situ* the relief of samples under load, a sample tensile device was installed directly in the AFM workspace. The resulting AFM-images had a lateral resolution of 512×512 points (per scan area), additionally converted into three-dimensional numerical arrays, which were used for statistical analysis.

3. Results and discussion

According to measurements of LEED patterns (Fig. 1), most of the surface of the Mo foil in the initial state is occupied by the dominant facet (100). The surface consists of individual blocks with dimensions of the order of the cross section of the analyzing electron beam (hundreds of μm). The Int-LEED [20] method was additionally used to analyze the morphological changes of the loaded molybdenum foil surface in UHV. The samples were subjected to uniaxial tension up to a load of ~ 400 MPa, at which the failure of the sample occurred. Figure 1 shows the LEED and Int-LEED patterns obtained in the initial and loaded states. The greatest change in LEED patterns

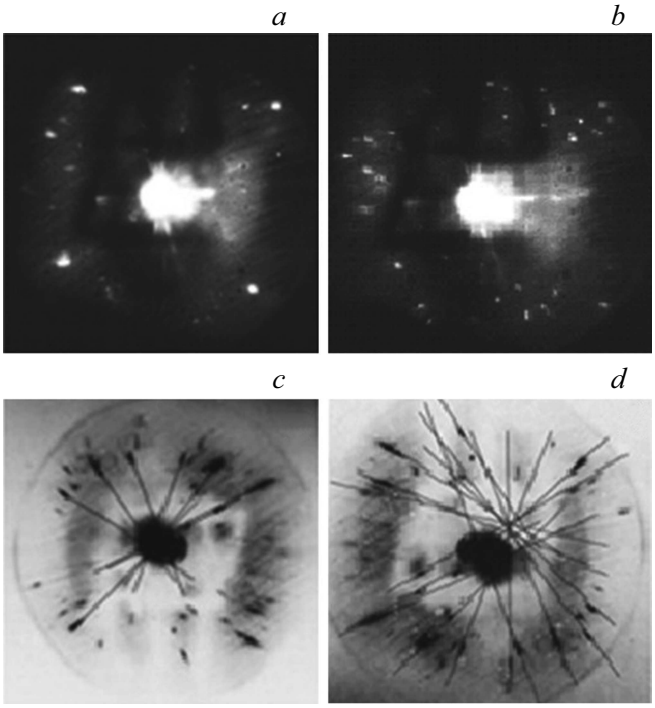

Figure 1. LEED and Int-LEED images from the Mo foil surface:*a* and *c* — $\sigma = 0$, *b* and *d* — $\sigma \sim 360$ MPa.

was observed at the sites of the upcoming sample rupture. Figure 1, *a* and 1, *c* correspond to the LEED and Int-LEED picture obtained at $\sigma = 0$. Figure 1, *b* and 1, *d* show the LEED and Int-LEED pattern obtained at $\sigma \sim 360$ MPa. It can be seen that mechanical loading leads to the appearance of small „extra“ reflexes, indicating the formation of small blocks [14]. Destruction of the facet (100) and the formation of small crystallites (diffractively disordered state) is observed. A similar phenomenon on the surface before fracture of thin W samples was described in [17], and is associated with amorphization of the surface and its partitioning into nanocrystals. Int-LEED (Fig. 1, *d*) shows that the intersection of the continuation of the stretched reflexes is about 10° away from the center of the mirrored beam, and the rotation of converging reflexes relative to the reflexes shown in Fig. 1, *a* is from 5 to 15°. This means that in addition to the destruction of the facet into small blocks, there is also their rotation relative to each other, both in the plane perpendicular to the surface of the foil and in the lateral direction.

The surface topography of molybdenum bands was investigated using the AFM method. Topograms of sample surfaces in the initial state, under load, and after rupture were taken. Figure 2 shows three fragments ($1000\,\text{nm} \times 1000\,\text{nm}$) of these areas as two-dimensional images. Fig. 2, *a* — corresponds to the unloaded surface, Fig. 2, *b* — surface at ~ 360 MPa, Fig. 2, *c* — surface after rupture in the area close to the rupture site. It can be seen that the surface topography changes under load (Fig. 2, *b*). Rectangular

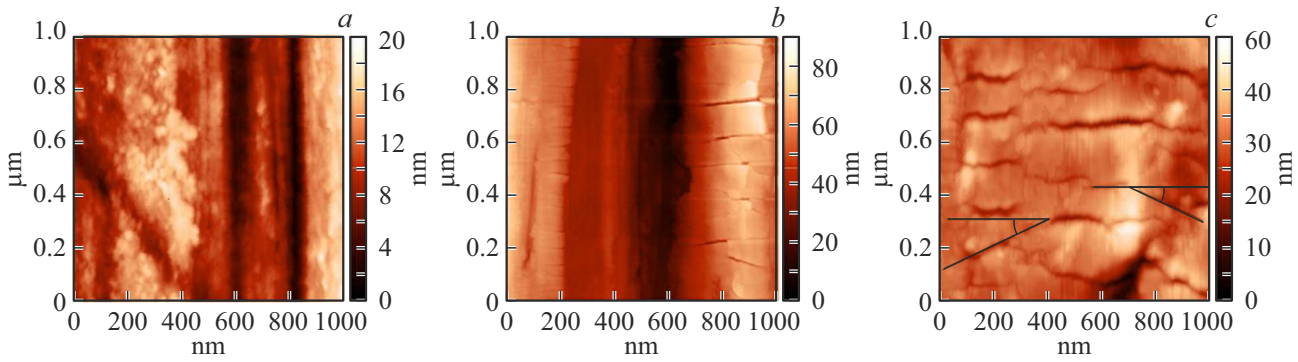

Figure 2. AFM-topograms of the Mo foil surface. Sample before loading (a), under $\sigma \sim 360$ MPa (b and after rupture (c).

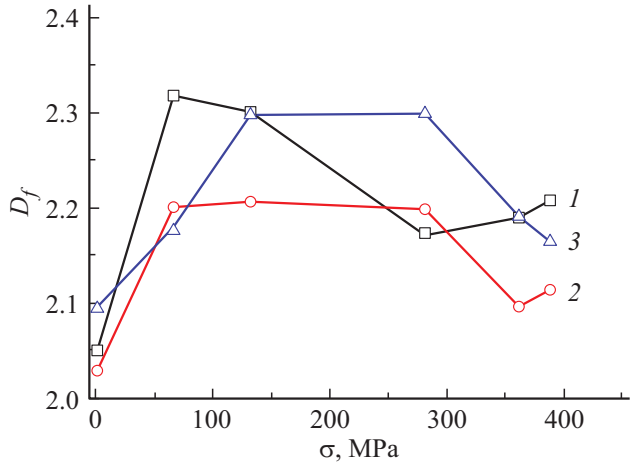

Figure 3. Dependence of the fractal dimension (D_f) on the stress applied to the sample (σ) for different surface areas: *1* — $1 \times 1\,\mu$m, *2* — $10 \times 10\,\mu$m, *3* — $30 \times 30\,\mu$m.

blocks of the order of 100 nm are formed, and some of them are disoriented in the lateral plane. In Fig. 2, *c* the surface is more fragmented, and there is also a more pronounced rotation of the blocks in the lateral plane.

It is likely that changes in the surface topography of the loaded and destroyed Mo band are associated with the processes of structural rearrangements occurring on the surface of the material under load.

For statistical analysis of the AFM-topograms of the surface, the fractal dimensions were calculated and the MFFC [15], method was applied, using the algorithm outlined in [16]. Dependences of the values of fractal dimensions (D_f) on the mechanical stress applied to the sample (σ) for different areas (*1, 2, 3*), are shown in Fig. 3. It can be seen that with increasing tensile load, the fractal dimension behaves non-monotonically. According to [19], as the load increases, the maximum values of fractal dimension shift from small to large lateral scales. Thus, in the samples in the pre-break state ($\sigma = 220$ MPa), at the largest scales ($100\,\mu$m^2), the values D_f reach a maximum, while at the smaller (previous level) scale ($9\,\mu$m^2) the value of D_f has already managed to decrease in comparison with the previous load (150 MPa). At an even smaller increase ($1\,\mu$m^2), the value of D_f experienced a maximum at the initial load ($\sigma = 25$ MPa). Thus, when tensile stress is applied, it is evident that surface structuring begins at small lateral scales and, as the load increases, affects larger ones.

The same surface areas in the same load range were analyzed using the MFFC method. As a result, the singularity spectra $f(\alpha)$ were obtained and their widths were determined for each site. For this purpose, the details of the local scaling of the analyzed topograms were revealed, which was performed according to the following algorithm. The surface was covered with a square lattice of size l. The height of the surface profile was chosen as a multifractal measure on this lattice. The probability of filling a square cell was determined by the average height of the profile (the sum of heights of points belonging to the given cell, normalized to the total sum of heights of the considered section of the surface profile). The statistical sum was calculated in the standard way. Then, the scaling exponents $\tau(q)$ were determined from it, from which the

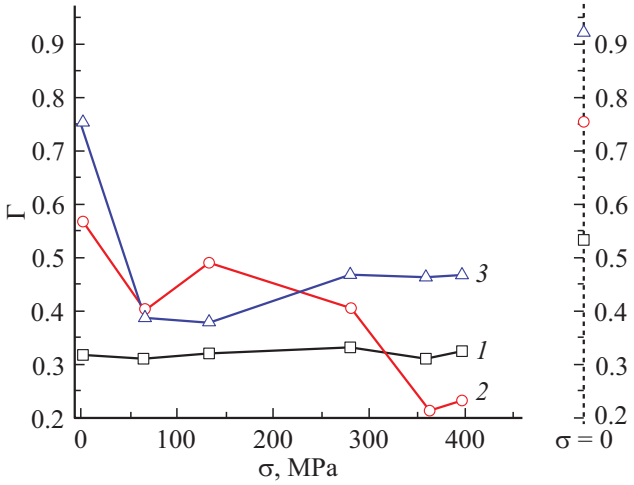

Figure 4. Dependence of singularity spectra widths (Γ) on the applied stress (σ) for different surface areas: *1* — $1 \times 1\,\mu$m, *2* — $10 \times 10\,\mu$m, *3* — $30 \times 30\,\mu$m.

desired spectrum $f(\alpha)$ was calculated. The calculation algorithm is described in detail in [11].

Figure 4 shows the values of the singularity spectra widths (Γ) depending on the applied tensile stress (σ).

It can be seen that as the sample approaches rupture, Γ begins to decrease. The dependence shows the tendency of the surface to monofractality, which may be a sign of an upcoming sample [17] rupture. It is important to note that after sample rupture Γ increases by a factor of $2-3$ for different sites. This is shown in the same figure on the ordinate axis to the right of Figure 4. The results in Fig. 4 show that the surface transitions to a multifractal state after the sample destruction.

4. Conclusion

Applying of mechanical stress leads to the destruction of the dominant edge (100) together with the rotation of surface layers blocks and small crystal formation in the Mo ribbon. Fragmentation of the surface structure in the lateral plane of the ribbon into ~ 100 nm areas was revealed, which is associated with the surface topography changes on other scales as well. It is shown that the external stress affects the fractal dimension and the formation of the sample surface scaling before rupture. In our opinion, the most informative sign of an incoming rupture is the narrowing of the width of the singularity spectrum, i.e. the tendency towards mono-fractalization of the surface. In the non-linear dynamics framework, this behavior is due to a change in the nature of the process from a more complex — multi-fractal to a simpler — mono-fractal, i.e., to fractal self-organization.

Conflict of interest

The authors declare that they have no conflict of interest.

References

[1] T.E. Smolyarova, A.V. Lukyanenko, A.S. Tarasov, L.V. Shanidze, F.A. Baron, F.V. Zelenov, I.A. Yakovlev, N.V. Volkov. J. Phys.: Conf. Ser. 1410, (2019). doi:10.1088/1742-6596/1410/1/012013.
[2] T.E. Smolyarova, L.V. Shanidze, A.V. Lukyanenko, F.A. Baron, V.V. Krasitskaya, A.S. Kichkailo, A.S. Tarasov, N.V. Volkov. Talanta **239**, 123092, (2022).
[3] Anil K. Battu, Nanthakishore Makeswaran, C.V. Ramana. J. Mater. Sci.Technol. **35**, *11*, 2734 (2019). https://doi.org/10.1016/j.jmst.2019.05.023.
[4] K. Prajwal, G.L. Priyanka, M.A. Hasan, A.C.M. Esther, N. Sridhara, A. Rajendra, S.B. Arya, A. Dey. Surf. Eng. **37**, *3*, 400 (2021).
[5] K. Radican, S.I. Bozhko, S.-R. Vadapoo, S. Ulucan, H.-C. Wu, A. McCoy, I.V. Shvets. Surf. Sci. **604**, *19–20*, 1548 (2010).
[6] U. Berner, K.D. Schierbaum. Phys. Rev. B **65**, *23*, 235404-1-10 (2002).
[7] Xinyi Dai, Aijun Zhou, Lidong Feng, Ying Wang, Jin Xu, Jingze Li. Thin Solid Films **567**, 64 (2014). https://doi.org/10.1016/j.tsf.2014.07.043.
[8] V.E. Korsukov, S.A. Knyazev, A.L. Buynov, M.M. Korsukova, S.A. Nemov, B.A. Obidov. Letters in ZhTF **39**, *8*, 55 (2013).
[9] S.A. Knyazev, V.E. Korsukov. FTT **47**, *5*, 876 (2005) (in Russian).
[10] R. Kaindi, B.C. Bayer, R. Resel, T. Muller, V. Skakalova, G. Habler, R. Abart, A.S. Cherevan, D. Eder, M. Blatter, F. Fischer, J.C. Meyer, D.K. Polyushkin, W. Waldhauser. Beilstein J. Nanotechnol. **8**, 1115 (2017). https://doi.org/10.3762/bjnano.8.113
[11] S.A. Smagulova, P.V. Vinokurov, A.A. Semenova, E.I. Popova, F.D. Vasilyeva, E.D. Obraztsova, P.V. Fedotov, I.V. Antonova. FTP **54**, *4*, 376 (2020) (in Russian). DOI: 10.21883/PSS.2022.08.54606.364
[12] Xiaoying Fu, Zenglin Zhou, Yan Li, Zhilin Hui, Xueliang He, Wenshuai Chen. Int. J. Ref. Met. Hard Mater. **93**, 105341 (2020). https://doi.org/10.1016/j.ijrmhm.2020.105341.
[13] Atanu Chaudhuri, Apu Sarkar, Satyan Suwas. Int. J. Ref. Met. Hard Mater. **73**, 168 (2018).
[14] V.E. Korsukov, S.A. Knyazev, A.V. Ankudinov, M.M. Korsukova, B.A. Obidov. Letters in ZhTF **40**, *6*, 35 (2014).
[15] T. Tel. Z. Naturforsch. **43**, *12*, 1154 (1988).
[16] M. Nasehnejad, M. Cholipour Shahraki, G. Nabiyouni. Appl. Surf. Sci. **389**, 735 (2016).
[17] V.E. Korsukov, A.V. Ankudinov, V.I. Betekhtin, P.N. Butenko, V.N. Verbitsky, V.L. Hilarov, I.V. Hilarov, S.A. Knyazev, M.M. Korsukova, B.A. Obidov. FTT **62**, *12*, 2003 (2020) (in Russian).
[18] V.E. Korsukov, A.V. Ankudinov, P.N. Butenko, S.A. Knyazev, M.M. Korsukova, B.A. Obidov, I.P. Shcherbakov. Letters in ZhTF **40**, *18*, 1 (2014).
[19] P.N. Butenko, V.L. Hilarov, V.E. Korsukov, A.V. Ankudinov, S.A. Knyazev, M.M. Korsukova, B.A. Obidov. FTT **63**, *10*, 1451 (2021).
[20] G.K. Ziryanov, S.A. Knyazev, V.P. Makhnyuk. Technical Physics **45**, *5*, 666 (1975).